Theoretical and Applied Mechanics Letters 5 (2015) 160–166

Contents lists available at ScienceDirect

Theoretical and Applied Mechanics Letters

journal homepage: www.elsevier.com/locate/taml

Will oscillating wave surge converters survive tsunamis?

L. O'Brien [a], P. Christodoulides [b], E. Renzi [c,d], T. Stefanakis [c,e], F. Dias [c,e,*]

[a] School of Mathematical Sciences, Monash University, Victoria 3800, Australia
[b] Faculty of Engineering and Technology, Cyprus University of Technology, Limassol, Cyprus
[c] School of Mathematical Sciences, University College Dublin, Belfield Dublin 4, Ireland
[d] Department of Mathematical Sciences, Loughborough University, Loughborough, Leics LE11 3TU, UK
[e] Centre de Mathématiques et de Leurs Applications (CMLA), Ecole Normale Supérieure de Cachan, 94235 Cachan, France

ARTICLE INFO

Article history:
Received 11 January 2015
Received in revised form
8 May 2015
Accepted 14 May 2015
Available online 9 June 2015
*This article belongs to the Fluid Mechanics

Keywords:
Tsunami
Wave energy converter
Wave loading
Oscillating wave surge converter
Wave-structure interaction

ABSTRACT

With an increasing emphasis on renewable energy resources, wave power technology is becoming one of the realistic solutions. However, the 2011 tsunami in Japan was a harsh reminder of the ferocity of the ocean. It is known that tsunamis are nearly undetectable in the open ocean but as the wave approaches the shore its energy is compressed, creating large destructive waves. The question posed here is whether an oscillating wave surge converter (OWSC) could withstand the force of an incoming tsunami. Several tools are used to provide an answer: an analytical 3D model developed within the framework of linear theory, a numerical model based on the non-linear shallow water equations and empirical formulas. Numerical results show that run-up and draw-down can be amplified under some circumstances, leading to an OWSC lying on dry ground!

1. Introduction

The estimation of the effects of tsunami-induced loading on near-shoreline structures located within inundation zones has recently gained significant interest from researchers, engineers, and government agencies [1,2]. Wave energy devices and tidal current turbines are slowly becoming a reality. Various prototypes are now being tested in harsh sea conditions, due for example to violent storms. The effectiveness of a mooring system to hold a turbine under extreme weather conditions has been examined for example by Chen and Lam [3]. Tiron et al. [4] provided a review on the challenges that wave energy devices face, in particular those associated with extreme wave events. What about tsunamis?

There was no wave energy converter (WEC) installed at the time of the March 11, 2011 Japan tsunami but there is some information available about offshore wind turbines. Simply structured wind-power plants proved more resistant to natural disasters than nuclear plants. For example the wind plant 50 m off the coast of Kamisu, Ibaraki Prefecture, survived the massive tsunami and continues to run at full capacity supplying electricity to Tokyo Electric Power Co., which was greatly compromised when the waves crippled the Fukushima No. 1 nuclear plant. The wind plant has seven power generators. Each generator is attached to three propeller blades sitting atop a mast that, when turning, transform wind into electricity. Each mast, sunk into the seabed at a depth of 25 m, stands roughly 70 m above the water. The tsunami reached 5 m. Each transformer is located on a jetty dozens of meters away from the masts. The machine stayed dry amid the tsunami because the jetty, connected to a coastal road, is 9.6 m above sea level and the walls and ceiling kept water from splashing onto the machine.

Even if offshore wind turbines seem to have survived the 2011 Japan tsunami, it is legitimate to ask whether WECs will resist tsunamis. In the future some WECs could be installed in areas prone to tsunamis (off the coasts of Oregon or Washington for example where a devastating Cascadia earthquake could generate a threatening tsunami). For the North Sea, the threat is not as obvious, even though O'Brien et al. [5] have indicated some possibilities for tsunamis. A large underwater landslide, called the Peach slide, took place on the Barra Fan, about 250 km off the North West coast of Ireland. It has a minimum age of 14680 years BP, was formed through a combination of blocky and muddy debris flows and affects an area of 700 km^2. A landslide of such proportion could very well have generated a large scale tsunami. The Storegga slide is one of the world's largest known submarine landslides and occurred off the west coast of Norway generating a huge

* Corresponding author at: School of Mathematical Sciences, University College Dublin, Belfield Dublin 4, Ireland.
E-mail address: laura.obrien@monash.edu (L. O'Brien).

http://dx.doi.org/10.1016/j.taml.2015.05.008

Fig. 1. Photo of the Pelamis wave power device [6]. The device is typically 1600 m from the shoreline.

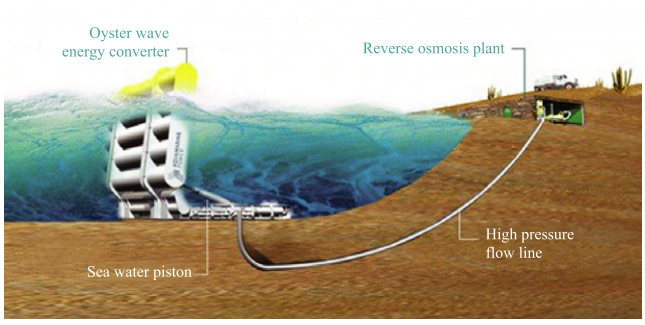

Fig. 2. Drawing of the Oyster wave power device [9]. The water depth is between 10 m and 13 m where the device is installed. The device is typically 500 m from the shoreline.

tsunami. Recent studies estimate that the slide removed between 2500 km^3 and 3500 km^3 of sediment from the slide scar approximately 8200 years BP. It is thought that inundation was as high as 30 m and reached Norway, Shetland, Scotland, and the Faroes. For deep sea WECs, such as Pelamis [6] (Fig. 1), or for current turbines usually installed at the sea bottom under at least 30 m of water, tsunamis are not anticipated to be a threat since they are located far from the shore (the present Pelamis prototype operating at EMEC [7], Orkney, is located 1.6 km from the shore and the present OpenHydro [8] project in Brittany, France, is located 2 km from the shore). On the other hand, for nearshore WECs, such as the oscillating wave surge converter (OWSC) Oyster [9] (Fig. 2), it is important to take a closer look at the effect of tsunamis (the present Oyster prototype operating at EMEC, Orkney, is located 500 m from the shore). Unfortunately there is very few tsunami wave data away from the shoreline. One exception is the Mercator yacht, anchored 1.6 km away from the shore in Thailand during the 2004 Indian Ocean tsunami. The water depth was about 12–13 m and the yacht experienced four major waves, one "depression" wave (2.8 m) and three "elevation" waves (3.8, 1.7, and 4.2) [10]. The problem of tsunami-induced loading is quite different from the problem of wave forces acting on flap-type storm surge barriers [11–13] because the periods involved are different. From the point of view of global wave loading, tsunamis are less of a threat than storm surges or extreme storm waves as shown below. However, there are some other issues, e.g., extreme rundown, wave impact after the OWSC has been left on dry ground, wave breaking on the OWSC.

St-Germain et al. [14] simulated the impact on structures of tsunami-like bores rapidly advancing on dry and wet beds. They used a 3D numerical model based on the smoothed particle hydrodynamics (SPH) method. The time-histories of the pressures and net force acting on a square column and a vertical wall due to the impact of these bores were compared qualitatively. To better understand the development of the hydrodynamic forces, a detailed analysis of the velocity field and of the water surface elevation was also incorporated. This study was part of a comprehensive interdisciplinary research program whose purpose was to help develop design guidelines for tsunami-prone structures.

Table 1
Dimensionless numbers.

Relative height	Wave shallowness	Wave steepness	Ursell number
$\epsilon_i = a_i/h_i$	$\delta_i = h_i/\lambda_i$	$\gamma_i = a_i/\lambda_i$	$Ur_i = \epsilon_i/\delta_i^2$

Until recently there has been very little emphasis on draw-downs. For obvious reasons, residents care more about run-ups! With the development of OWSCs, the focus is different. It is in the vicinity of the extreme draw-down location that the maximum momentum flux occurs [15].

For the methods, we use an analytical 3D model developed within the framework of linear theory by Renzi and Dias [16], numerical solutions based on the non-linear shallow water equations [17] and empirical formulas [18,19].

In Section 2, we briefly investigate the transformation of tsunami waves as they approach the shore. In Section 3, we present results based on an analytical model and we show that they do not allow us to conclude on the loading exerted by tsunamis. In Section 4, we discuss numerical results. In Section 5, we discuss the relevance of empirical formulas.

2. Tsunami wave transformation

The wave transformation during the final stage of the propagation of a tsunami has been described in several papers. A particularly clear example is the paper of Madsen and Fuhrman [19]. Kajiura [20] considers the amplification of tsunamis which advance towards shore over a gentle slope using Green's law for tsunamis

$$\frac{a_1}{a_2} = \left(\frac{\lambda_2}{\lambda_1}\right)^{\frac{1}{2}} = \left(\frac{h_2}{h_1}\right)^{\frac{1}{4}}, \tag{1}$$

where a_i and λ_i are the amplitude and wavelength of a tsunami at a depth h_i, at two different positions $i = 1, 2$. More interesting in the framework of the present study is the amplification of velocity and consequently of the momentum flux per unit breadth $f_i = h_i u_i^2$. Since u_i scales as $a_i\sqrt{(g/h_i)}$ in linear shallow water theory

$$\frac{u_1}{u_2} = \left(\frac{\lambda_2}{\lambda_1}\right)^{\frac{3}{2}} = \left(\frac{h_2}{h_1}\right)^{\frac{3}{4}}, \qquad \frac{f_1}{f_2} = \frac{h_1 u_1^2}{h_2 u_2^2} = \left(\frac{h_2}{h_1}\right)^{\frac{1}{2}}. \tag{2}$$

If the water depth is reduced by half between two points, the wave height increases by 19% while the momentum flux increases by 41%. As stated by Carrier et al. [15], f can be interpreted as the drag force per unit breadth for a surface-piercing stationary object placed vertically over the flow depth.

In order to assess the importance of linear, non-linear and dispersive effects, four dimensionless parameters are defined in Table 1.

Eq. (1) implies that these dimensionless numbers are transformed as follows:

$$\begin{aligned} \frac{\epsilon_1}{\epsilon_2} &= \left(\frac{h_2}{h_1}\right)^{5/4}, \qquad \frac{\delta_1}{\delta_2} = \left(\frac{h_2}{h_1}\right)^{-1/2}, \\ \frac{\gamma_1}{\gamma_2} &= \left(\frac{h_2}{h_1}\right)^{3/4}, \qquad \frac{Ur_1}{Ur_2} = \left(\frac{h_2}{h_1}\right)^{9/4}. \end{aligned} \tag{3}$$

For a large tsunami wave with $a_1 = 1$ m, $h_1 = 3$ km, $\lambda_1 = 100$ km, the transformation of the dimensionless parameters arising from Table 1 is shown in Table 2 for two depths: 30 m and 10 m.

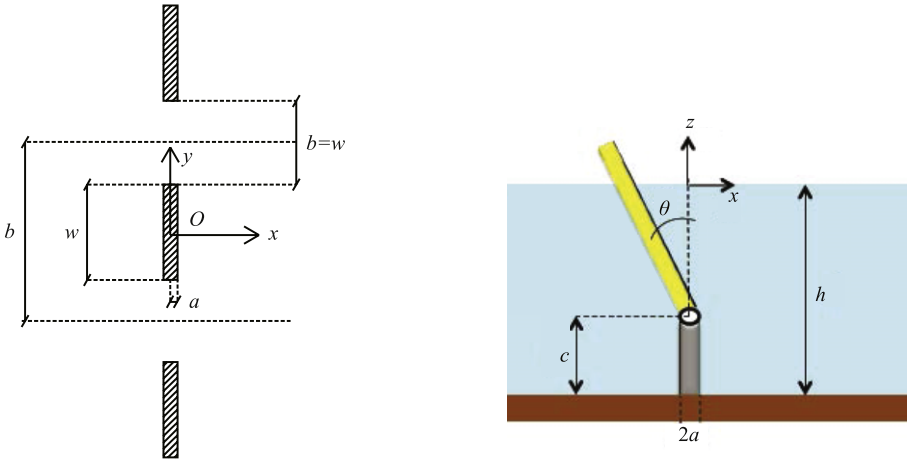

Fig. 3. Geometry of the array of OWSCs: plan view (left) and side view (right).

Table 2
Transformation of dimensionless numbers for a tsunami at three positions according to Eq. (3).

	$h = 3$ km	$h = 30$ m	$h = 10$ m
ϵ_i	3.3×10^{-4}	0.11	0.42
δ_i	3×10^{-2}	3×10^{-3}	1.7×10^{-3}
γ_i	1.0×10^{-5}	3.2×10^{-4}	7.2×10^{-4}
Ur_i	0.37	1.2×10^{4}	1.4×10^{5}

The values of relative height ϵ indicate that linear theory can be used to describe the behavior of the wave up to a certain depth and the values of wave shallowness δ suggest that slight dispersive effects should be included for waves traveling over very large distances. As the wave approaches the shore, finite amplitude (non-linear) effects come into play when the relative height $\epsilon \approx 10^{-1}$. According to Eq. (3) this occurs at a depth slightly larger than $h = 30$ m. Assuming a seabed slope of 0.02 this occurs at a distance of approximately 1.5 km from the shore, which is about 1/7 of the wavelength of a tsunami with a period of 10 min. The dimensionless parameters corresponding to $h = 30$ m are shown in column 2 of Table 2. The wave steepness is $\gamma \approx 0.0003$ and the Ursell number is $Ur \approx 10^4 \gg 1$, indicating that dispersion is relatively minor compared with the non-linearity except for the front part of the wave. From these considerations, it is reasonable to conclude that at this distance from the shore there is a shift in importance from linear to non-linear effects. Therefore, linear shallow-water equations used offshore should be matched to the inner solution of the non-linear shallow-water equations at a distance from shore of about 1/7 of a wavelength of the tsunami. At a depth of 10 m, the situation is even worse. The dimensionless parameters corresponding to $h = 10$ m are shown in column 3 of Table 2.

In the next section, linear theory is used as a first approximation to predict the force exerted on an OWSC. It will be shown in Section 4 that as anticipated the linear results underestimate the force and that it is necessary to use non-linear theory.

3. Linear theory

We consider here the following idealized problem: a flap-type structure mounted on a flat sea bottom pierces the surface of the ocean. The structure is assumed to be fixed. The loading on the flap due to a tsunami wave is estimated. The most restrictive assumption is that the bottom is flat.

The analytical 3D model developed by Renzi and Dias [16] is used to compute the load on the flap. This is the same model that is implemented to determine the hydrodynamic loading on an array of OWSCs in random seas [21–23]. Until now, this model had only been used to compute forces under normal operational conditions for OWSCs, that is waves with periods between 5 s and 20 s. Even though there is no assumption on the wave period in the derivation of the model, special care must be taken when evaluating the solution for long waves.

Let us consider an infinite array of equally spaced thin plates in the open ocean used for the purpose of wave energy conversion. The analysis of the scattering problem, in which the flaps are held fixed in incoming waves, is used here to calculate the velocity potential and so, the pressure exerted on the system. This is important in order to investigate whether an array of nearshore OWSCs would survive the impact from a tsunami. Periodicity of the problem allows the geometry to be reduced to that of a single plate within two waveguides at a mutual distance b, as shown in Fig. 3.

With reference to Fig. 3, the plate is represented by a rectangular box of width w and thickness $2a$, fixed along a straight foundation at a distance c from the bottom of the ocean of depth h. The plate is in the middle of a channel of total width b. A plane reference system of coordinates $\boldsymbol{x} = (x, y, z)$ is also set, with x on the center line of the channel, y along the axis of the plate, and z positive upwards. Monochromatic waves of frequency ω are incoming from the left with wave crests parallel to the plate.

The theoretical basis of the mathematical model is provided by Renzi and Dias [16] and summarized here. Within the framework of a linear potential-flow theory, the velocity potential $\Phi(x, y, z, t)$ must satisfy the Laplace equation

$$\nabla^2 \Phi(x, y, z, t) = 0 \tag{4}$$

in the fluid domain. On the free-surface, the kinematic-dynamic boundary condition

$$\frac{\partial^2 \Phi}{\partial t^2} + g \frac{\partial \Phi}{\partial z} = 0, \quad z = 0 \tag{5}$$

is applied, with g being the acceleration due to gravity. Absence of normal flux at the bottom and through the lateral walls of the channel requires

$$\frac{\partial \Phi}{\partial z} = 0, \quad z = -h, \qquad \frac{\partial \Phi}{\partial y} = 0, \quad y = \pm b/2, \tag{6}$$

respectively.

A no-flux boundary condition must be applied on the lateral surfaces of the fixed plate, yielding

$$\frac{\partial \Phi}{\partial x} = 0, \quad x = \pm a, \ |y| < w/2. \tag{7}$$

Since the total thickness of the plate $2a \ll b$, the thin-plate approximation can be used [24] by which the boundary condition on the plate (7) is restated at $x = \pm 0$. Finally, the reflected and transmitted wave field respectively on the weather side and the lee side of the plate must be both outgoing at large distances from the origin.

The system of governing equations (4)–(7) can be solved via the introduction of a complex spatial potential such that

$$\Phi = \Re\left\{[\phi_{\mathrm{I}}(x, y, z) + \phi_{\mathrm{D}}(x, y, z)]\mathrm{e}^{-\mathrm{i}\omega t}\right\}. \tag{8}$$

The velocity potential physically represents oscillating waves of period $T = 2\pi/\omega$, whose spatial variation is described by the sum of two different components, ϕ_{I} and ϕ_{D}. The first term, ϕ_{I}, represents the *incident* wave field and is given by

$$\phi_{\mathrm{I}}(x, y, z) = -\frac{\mathrm{i}Ag}{\omega \cosh(kh)} \cosh[k(z + h)]\mathrm{e}^{-\mathrm{i}kx}, \tag{9}$$

where A and k are respectively the wave amplitude and wavenumber, the latter depending on the wave frequency according to the dispersion relation $\omega^2 = gk \tanh(kh)$.

The full solution (for details see Refs. [16,25]) of (4)–(7) is based on a careful application of the Green integral theorem in the fluid domain. Herein we report the corresponding semi-analytical solution and its physical meaning. Eq. (9) describes a monochromatic wave field. Incident monocromatic waves can describe the fundamental behavior of the flap. Referring to Eq. (8), ϕ_{D} is the *diffraction* potential that describes the modification of the wave field induced by the physical presence of the flap held fixed in water. The mathematical expression of ϕ_{D}, not reported here for the sake of brevity, can be found in Ref. [25].

The force of a tsunami on an array of nearshore OWSCs at a depth of 10.9 m is analyzed. If the tsunami has an amplitude of 1 m offshore at a depth of 3 km, then according to Green's law for tsunamis (1) the amplitude of the wave will be approximately 4 m when it hits the devices. As said above, in order to analyze the tsunami effect on the system, we approximate the OWSCs as an array of fixed plates with a spatial period $b = 91.6$ m and width $w = 18$ m and determine the pressure exerted on one plate from a tsunami with amplitude 4 m and period 10 min. In the linear model $p = -\rho(gz + \Phi_t)$, the force exerted on the plate is determined by the pressure difference across the plate. We focus here on the dynamic pressure $-\rho\Phi_t$. The pressure jump across the plate is shown in Fig. 4. It is plotted against y which runs along the axis of the plate and calculated at six equally spaced depths from the still water level to the sea floor. The greatest overall pressure difference is felt at the center of the plate ($y = 0$) and is zero at the edges of the plate ($y = \pm 9$ m) but is invariant with depth. The maximum value is $\Delta P \approx 3 \times 10^3$ N/m^2 $= 0.03$ bar.

In order to compare these results to a standard sea state, the pressure jump exerted by a typical swell with amplitude 3 m and period 5 s impacting on the plate is shown in Fig. 5. This clearly shows how the pressure changes with depth: the maximum effect is felt at the free surface and the pressure decreases towards the sea floor. Also the magnitude is much greater than that from the tsunami, with a maximum $\Delta P \approx 3 \times 10^5$ N/m^2 $= 3$ bar. From these results we can conclude that the tsunami load exerted on the plate does not vary with depth since it is such a long wave relative to the depth. Moreover, the magnitude of load exerted by the tsunami is approximately 100 times less than that of a normal swell. We can therefore assume that an array of nearshore OWSCs would easily withstand the force from a tsunami according to linear theory. However, as previously noted, non-linear effects will start to become important at approximately 1.5 km from the shore so non-linear effects on the plate will be investigated in the next section.

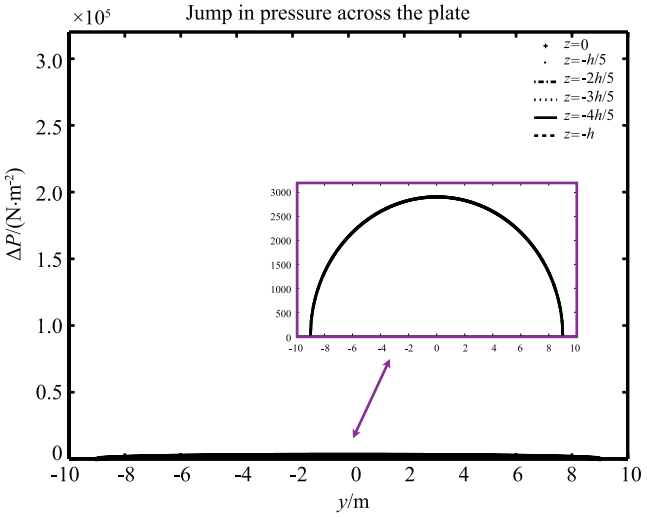

Fig. 4. The jump in pressure for a typical tsunami across an 18 m plate, in a depth of $h = 10.9$ m at six depths from the free surface to the ocean floor.

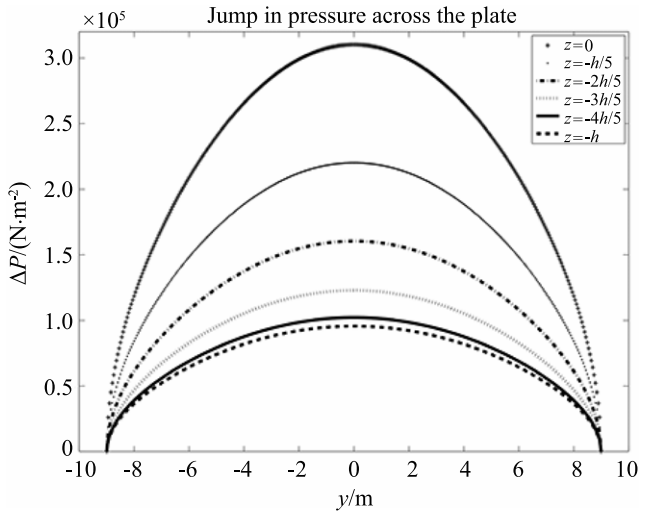

Fig. 5. Various jumps in pressure across an 18 m plate for a typical swell. (The same scales have been used in Figs. 4 and 5.)

4. Beyond linear theory

The (1D) fully non-linear shallow water equations read

$$\frac{\partial \eta}{\partial t} + \frac{\partial}{\partial x}[(h + \eta)\, u] = 0, \qquad \frac{\partial u}{\partial t} + u\frac{\partial u}{\partial x} + g\frac{\partial \eta}{\partial x} = 0. \tag{10}$$

Consider a topography consisting of a sloping beach with unperturbed water depth varying linearly with the horizontal coordinate, $h(x) = -\alpha x$. Carrier et al. [15] carefully evaluated tsunami run-up and draw-down motions on such a uniformly sloping beach. They considered several types of initial conditions. Kânoğlu [26] proposed an elegant alternative, which avoids the difficulty with the Carrier–Greenspan transformation, namely the derivation of an equivalent initial condition over the transform space for a given initial wave profile in the physical space.

Simply by looking at Ref. [15], one can make some interesting comments:

One sees that a flap mounted in water depths of the order of 10 m will not become dry but it could be close (with a rundown of 8 m).

It was shown in the previous section on linear theory that the forces due to the linear term $\partial\Phi/\partial t$ can be neglected. On the other

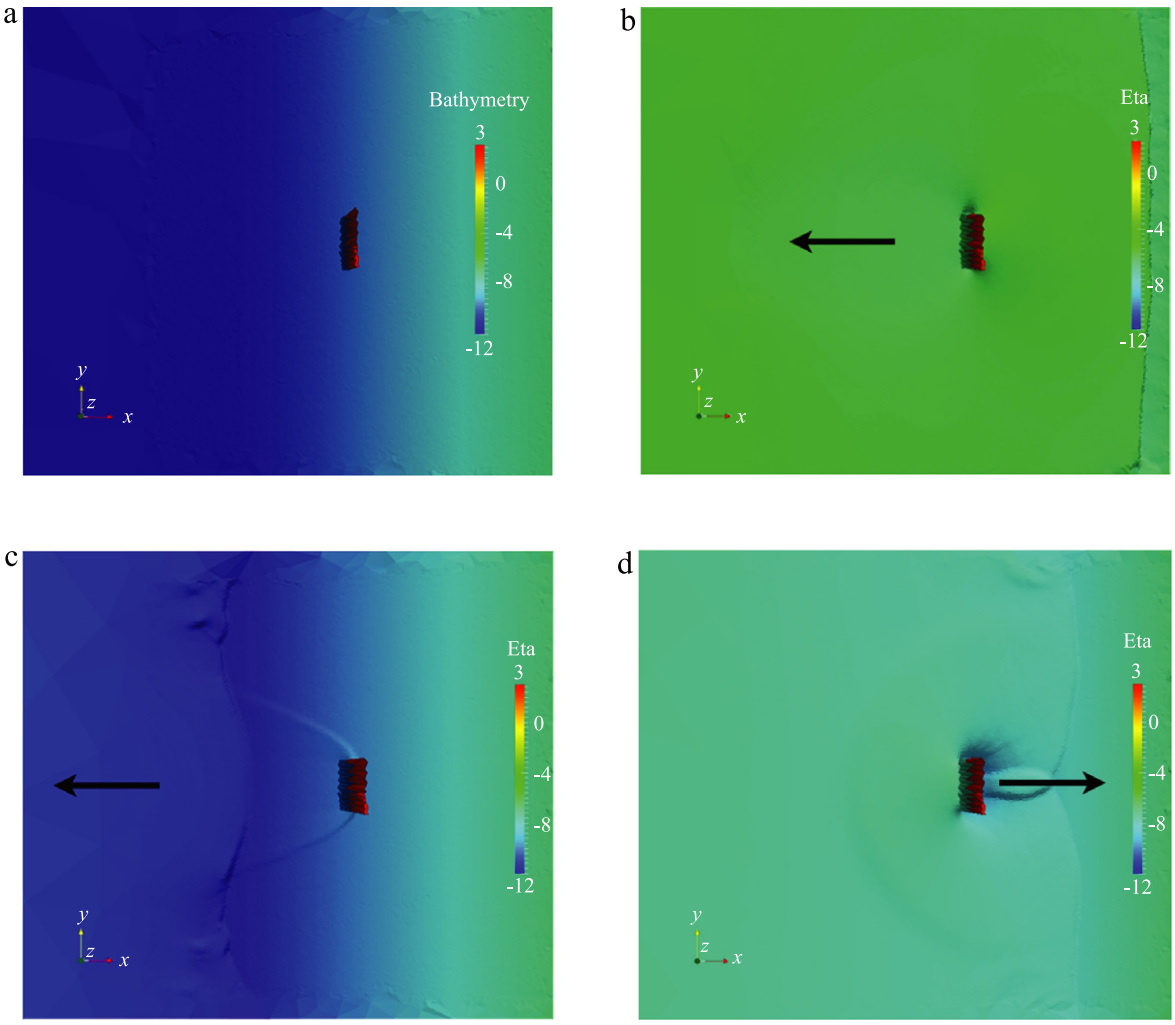

Fig. 6. VOLNA simulation from multiple tsunami waves hitting a 13 m high plate in an initial depth of 10 m on a sea bed with slope 0.03 (plane view). (a) Bathymetry of a fixed plate on a sloping sea bed with the shore to the right of the plate. (b) The free surface η after a tsunami has inundated the shore and it begins to recede. (c) 45 s later, the plate is left on dry land. (d) Another 45 s later, a subsequent wave impacts the plate.

hand, the velocities can become quite large and the linearized approach can fail. A simple analysis provided by Madsen and Fuhrman [19] shows that maximum flow velocities of the order of 9 m/s can be reached. Consequently the kinetic energy can be quite large. Since the pressure in the fully non-linear model includes a term proportional to u^2, the forces can be quite large. Of course the bottom slope is an important parameter. A steep slope will provide smaller maximum flow velocities.

Carrier et al. [15] state that one of the drawbacks of their method is that it is only applicable for the problems in one spatial dimension with a uniformly sloping beach. Therefore we also used a two dimensional non-linear shallow water solver, VOLNA [27], to perform additional simulations. If after the first wave recedes the device is left on dry land, a second wave may act as a shock on the plate and do more damage than it would to a partially submerged device. This effect is demonstrated in Fig. 6.

5. Empirical formulas

Authorities tend to classify the different forces acting on a structure due to a tsunami in the following way [28–32]:

- Hydrostatic Forces: Occur when standing or slowly moving water encounters a structure. They are caused by an imbalance of pressure due to a differential water depth on opposite sides of structure and act perpendicular to the surface.
- Buoyancy Forces: Concern structures with little resistance to lift such as light wood frame buildings, basements, or swimming pools. These act vertically through the center of mass of the displaced volume.
- Hydrodynamic Forces: Caused by water flowing at a moderate to high velocity around a structure. These are a combination of the lateral forces caused by the pressure forces from the moving mass of water and the friction forces generated as the water flows around the structure. They include frontal impact, drag along the sides, and suction on the downstream side. These forces depend on flow velocity, fluid density, and structural geometry.
- Surge Force: Another variety of hydrodynamic force caused by the leading edge of a surge of a tsunami impinging on a structure.
- Impact Force: Results from debris or any object transported by floodwaters, striking against a structure.

Assuming that the load is mainly hydrodynamic, even within this idealized framework it is not clear what the main force is going to be. The loading for a solid wall facing the shoreline suggested by Yeh et al. [28] (ignoring impact forces and breaking wave forces) is given by the surge force

$$F_s = 4.5\rho g h^2 w, \tag{11}$$

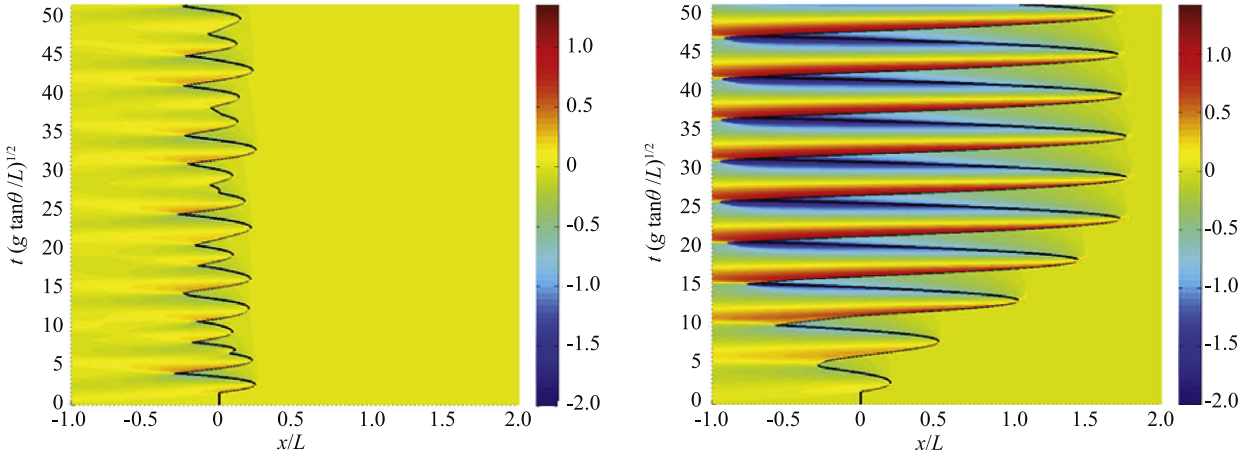

Fig. 7. Non-resonant (left) and resonant (right) non-dimensional velocities from a monochromatic wave on a sloping beach with slope $\tan\theta = 0.13$ and initial shoreline at $x = 0$ [35]. L is the distance from the shoreline to the point where the bottom becomes horizontal.

or the hydrodynamic force

$$F_{\mathrm{d}} = \frac{1}{2}\rho C_{\mathrm{d}} A u_{\mathrm{p}}^2, \tag{12}$$

where ρ is the water density, g is the acceleration due to gravity, w is the width of the wall, A is the area of the wall, h is the surge height, $C_{\mathrm{d}} \approx 1.5$ is the drag coefficient, and $u_{\mathrm{p}} = 2\sqrt{gh}$ is the design flood velocity.

A comparison of the above empirical formulas for a plate of width 18 m and a surge of height 10 m gives $F_{\mathrm{s}} = 8.1 \times 10^7$ N and $F_{\mathrm{d}} = 5.4 \times 10^7$ N. Both values are of the same order of magnitude and two order of magnitude larger than the force obtained with linear theory.

6. Conclusions

The hydrodynamic load of a tsunami on an array of nearshore OWSCs was investigated. The main conclusion is that non-linear theory must be used. Different forces suggested by standard tsunami design codes were reviewed displaying the variety of formulas and their reliance on estimated coefficients and a conservative velocity estimate. Applying the linear model of Renzi and Dias [16] to an array of fixed plates, a first approximation for the hydrodynamic loading on an OWSC was calculated through determining the jump in the $-\rho\Phi_t$ term. Results showed that the loading for a typical tsunami is invariant with depth and maximum loading is felt at the center of the plate. By comparison with the loading from a typical swell, it was shown that the maximum net force of a tsunami on a nearshore OWSC is approximately one hundredth of the magnitude of the loading due to a regular sea state. This paradox arises because the linearized theory neglects high-order hydrodynamic forces, which are dominant in a tsunami. However, further research needs to be done on the effects of multiple waves. Stefanakis et al. [33,34] demonstrated resonant phenomena between the incident wavelength and the beach slope within the framework of the non-linear shallow water equations in one dimension for multiple tsunami waves. A comparison between the velocities of resonant and non-resonant states from Stefanakis et al. [35] is shown in Fig. 7. Furthermore, if after the first wave recedes the device is left on dry land, a second wave may act as a shock on the plate and do more damage than it would to a partially submerged device. We believe that dangerous configurations could be found with more detailed investigations.

Acknowledgments

The authors would like to acknowledge the support provided by the Science Foundation Ireland (SFI) under the project High-end computational modeling for wave energy systems, by the Framework Program for Research, Technological Development, and Innovation of the Cyprus Research Promotion Foundation under the Project AΣTI/0308(BE)/05, by the Irish Research Council for Science Engineering and Technology (IRCSET), by Aquamarine Power and by the European Union's Seventh Framework Programme for research, technological development and demonstration under the grant agreement ASTARTE No. 603839.

References

[1] D. Palermo, I. Nistor, Y. Nouri, A. Cornett, Tsunami loading of nearshore structures: a primer, Can. J. Civil Eng. 36 (2009) 1804–1815. http://dx.doi.org/10.1139/L09-104.
[2] Y. Nouri, I. Nistor, D. Palermo, A. Cornett, Experimental investigation of the tsunami impact on free standing structures, Coast. Eng. J. 52 (1) (2010) 43–70. http://dx.doi.org/10.1142/S0578563410002117.
[3] L. Chen, W.-H. Lam, A review of survivability and remedial actions of tidal current turbines, Renew. Sustain. Energy Rev. 43 (2015) 891–900. http://dx.doi.org/10.1016/j.rser.2014.11.071.
[4] R. Tiron, F. Mallon, F. Dias, E.G. Reynaud, The challenging life of wave energy devices at sea: A few points to consider, Renew. Sustain. Energy Rev. 43 (2015) 1263–1272. http://dx.doi.org/10.1016/j.rser.2014.11.105.
[5] L. O'Brien, J.M. Dudley, F. Dias, Extreme wave events in Ireland: 14 680 BP - 2012, Nat. Hazards Earth Syst. Sci. 13 (3) (2013) 625–648. http://dx.doi.org/10.5194/nhess-13-625-2013. URL http://www.nat-hazards-earth-syst-sci.net/13/625/2013/.
[6] Pelamis. www.pelamiswave.com, 2015.
[7] EMEC. www.emec.org.uk, 2015.
[8] OpenHydro. www.openhydro.com, 2015.
[9] Aquamarine. www.aquamarinepower.com, 2015.
[10] T. Rossetto, W. Allsop, I. Charvet, D. Robinson, Physical modelling of tsunami using a new pneumatic water wave generator, Coast. Eng. 58 (2011) 517–527. http://dx.doi.org/10.1016/j.coastaleng.2011.01.012.
[11] P. Sammarco, H.H. Tran, C.C. Mei, Subharmonic resonance of Venice gates in waves. Part 1. Evolution equation and uniform incident waves, J. Fluid Mech. 349 (1997) 295–325. http://dx.doi.org/10.1017/S0022112097006848. URL http://journals.cambridge.org/article_S0022112097006848.
[12] P. Sammarco, H.H. Tran, O. Gottlieb, C.C. Mei, Subharmonic resonance of Venice gates in waves. Part 2. Sinusoidally modulated incident waves, J. Fluid Mech. 349 (1997) 327–359. http://dx.doi.org/10.1017/S0022112097006836. URL http://journals.cambridge.org/article_S0022112097006836.
[13] T. Tomita, K. Shimosako, T. Takano, Wave forces acting on flap-type storm surge barrier and waves transmitted on it, in: Proc.13th Int. Offshore and Polar Engineering Conf., Honolulu, Hawaii, USA, 2003, pp. 639–646.
[14] P. St-Germain, I. Nistor, R. Townsend, Numerical modeling of the impact with structures of tsunami bores propagating on dry and wet beds using the SPH method, Int. J. Protective Structures 3 (2) (2012) 221–255. http://dx.doi.org/10.1260/2041-4196.3.2.221.

[15] G.F. Carrier, T.T. Wu, H. Yeh, Tsunami run-up and draw-down on a plane beach, J. Fluid Mech. 475 (2003) 79–99. http://dx.doi.org/10.1017/S0022112002002653.
[16] E. Renzi, F. Dias, Resonant behaviour of the oscillating wave surge converter in a channel, J. Fluid Mech. 701 (2012) 482–510. http://dx.doi.org/10.1017/jfm.2012.194. URL http://journals.cambridge.org/article_S0022112012001942.
[17] F. Dias, D. Dutykh, L. O'Brien, E. Renzi, T. Stefanakis, On the modelling of tsunami generation and tsunami inundation, in: Procedia IUTAM, vol. 10, pp. 338–355 (2014). http://dx.doi.org/10.1016/j.piutam.2014.01.029.
[18] L. O'Brien, P. Christodoulides, E. Renzi, D. Dutykh, F. Dias, The force of a Tsunami on a Wave Energy Converter, in: Proceedings of the Twenty-second International Offshore and Polar Engineering Conference, Rhodes, Greece, vol. 1, June 17th–23rd (2012).
[19] P.A. Madsen, D.R. Fuhrman, Run-up of tsunamis and long waves in terms of surf-similarity, Coast. Eng. 55 (2008) 209–223. http://dx.doi.org/10.1016/j.coastaleng.2007.09.007.
[20] K. Kajiura, Local Behaviour of Tsunamis, in: D. Provis, R. Radok (Eds.), In Waves on Water of Variable Depth, in: Lecture Notes in Physics, vol. 64, Springer-Verlag, Berlin, 1977, pp. 72–79.
[21] E. Renzi, L. O'Brien, F. Dias, Hydrodynamic loading on an array of oscillating wave surge converters in random seas. In: Proceedings of the Twenty-second International Offshore and Polar Engineering Conference, Rhodes, Greece, vol. 1, pp. 663–668, June 17th–23rd (2012).
[22] D. Sarkar, E. Renzi, F. Dias, Wave power extraction by an oscillating wave surge converter in random seas, in: Proceedings of the 32nd International Conference on Ocean, Offshore and Arctic Engineering, Nantes, France, 2013.
[23] D. Sarkar, E. Renzi, F. Dias, Wave farm modelling of oscillating wave surge converters, Proc. R. Soc. A 470 (2014) 20140118. http://dx.doi.org/10.1098/rspa.2014.0118.
[24] C.M. Linton, P. McIver, Mathematical Techniques for Wave/Structure Interactions, Chapman & Hall/CRC, 2001.
[25] E. Renzi, F. Dias, Hydrodynamics of the oscillating wave surge converter in the open ocean, Eur. J. Mech. B Fluids 41 (2013) 1–10. http://dx.doi.org/10.1016/j.euromechflu.2013.01.007.
[26] U. Kânoğlu, Nonlinear evolution and runup-rundown of long waves over a sloping beach, J. Fluid Mech. 513 (2004) 363–372. http://dx.doi.org/10.1017/S002211200400970X. ISSN 1469-7645.
[27] D. Dutykh, R. Poncet, F. Dias, The VOLNA code for the numerical modeling of tsunami waves: Generation, propagation and inundation, Eur. J. Mech. B Fluids 30 (6) (2011) 598–615. http://dx.doi.org/10.1016/j.euromechflu.2011.05.005.
[28] H. Yeh, I. Robertson, J. Preuss, Development of Design Guidlines for Structures that Serve as Tsunami Vertical Evacuation Sites, Technical Report, Washington Division of Geology and Earth Resources, November 2005.
[29] Federal Emergency Management Agency, FEMA Coastal Construction Manual, 2000.
[30] ASCE Minimum Design Loads for Buildings and Other Structures, vol. ASCE 7-98, American Society of Civil Engineers, 1998.
[31] City and County of Honolulu Building Code, Department of Planning and Permitting of Honolulu Hawaii, July 2000.
[32] Dames and Moore, Design and Construction Standards for Residential Construction in Tsunami-prone Areas in Hawaii. Dames & Moore, 1980.
[33] T. Stefanakis, F. Dias, D. Dutykh, Local run-up amplification by resonant wave interactions, Phys. Rev. Lett. 107 (2011). http://dx.doi.org/10.1103/PhysRevLett.107.124502.
[34] T.S. Stefanakis, S. Xu, D. Dutykh, F. Dias, Run-up amplification of transient long waves, Quart. Appl. Math. 73 (2015) 177–199. http://dx.doi.org/10.1090/S0033-569X-2015-01377-0.
[35] T.S. Stefanakis, F. Dias, D. Dutykh, Resonant long-wave run-up on a plane beach, in: Proceedings of the Twenty-second International Offshore and Polar Engineering Conference, Rhodes, Greece, vol. 3, June 17th–23rd (2012).